Heat Transfer Experiments of Ribbed, Serpentine Cooling Passages with Supercritical CO_2

Michael Marshall, SwRI
Mark Anguiano, SwRI (presenter)
Jeff Moore, SwRI

Acknowledgement

- Work completed under the project, “Development of Coal Syngas Oxy-Combustion Turbine for Use in Advanced sCO_2 Power Cycles”, sponsored by the U.S. Department of Energy (FE-0031929).

Introduction – Direct Fired sCO_2 Cycles

- Direct-fired sCO_2 power cycles featuring oxy-combustion are a promising technology due to the ability to have near zero CO_2 emissions while achieving competitive plant efficiencies on the utility scale.
- Past system studies on the Allam-Fetvedt cycle have predicted a 53% LHV net efficiency for a plant utilizing natural gas [1], and a 42% LHV net efficiency for a plant utilizing coal syngas fuel [2].

Introduction – Turbine Blade Details

- Direct-fired sCO_2 turbines have an inlet temperature exceeding 1100°C, necessitating internally cooled blades.
- Cooling blade schemes can mirror that of a gas turbine:
  - Impingement cooling in the leading edge region.
  - **Serpentine cooling in the blade mid-section.**
  - Pin-fin cooling in the trailing edge region.

Introduction – Mid-section serpentine cooling

- Due to the high density, low viscosity of sCO_2, Reynolds (RE) numbers can exceed those in typical air-breathing turbine cooling by an order of magnitude.
  - Numerous studies have been conducted with air under RE numbers of 100,000.
  - Studies with sCO_2 have shown an angled ribbed passage at RE near 140,000 with a Nusselt number enhancement ratio (Nu/Nu_0) between 2.6 and 3.0.
- The test campaign sought to gain heat transfer data for a geometry that included ribbed passage lengths with 180 deg. tip turns, for conditions in sCO_2 that were representative of those to be seen in the end oxy-fuel turbine application

Test Loop Setup

- Testing leverages a 1 MWe scale test loop at SwRI:
  - Primary heater outlet (Hot Flow).
  - Recuperator outlet (Cooling Flow).
  - Compressor discharge.

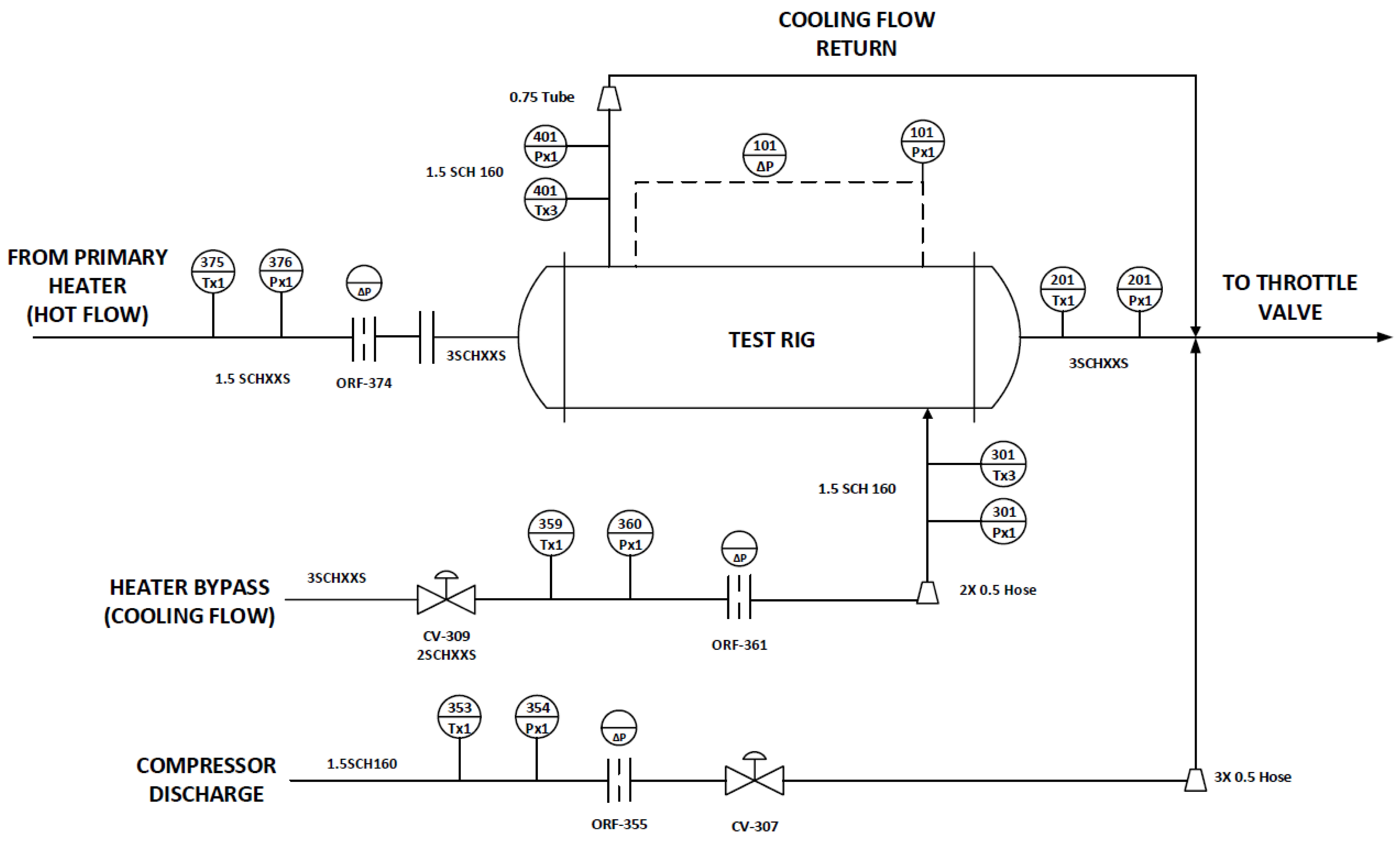

Test Loop Setup

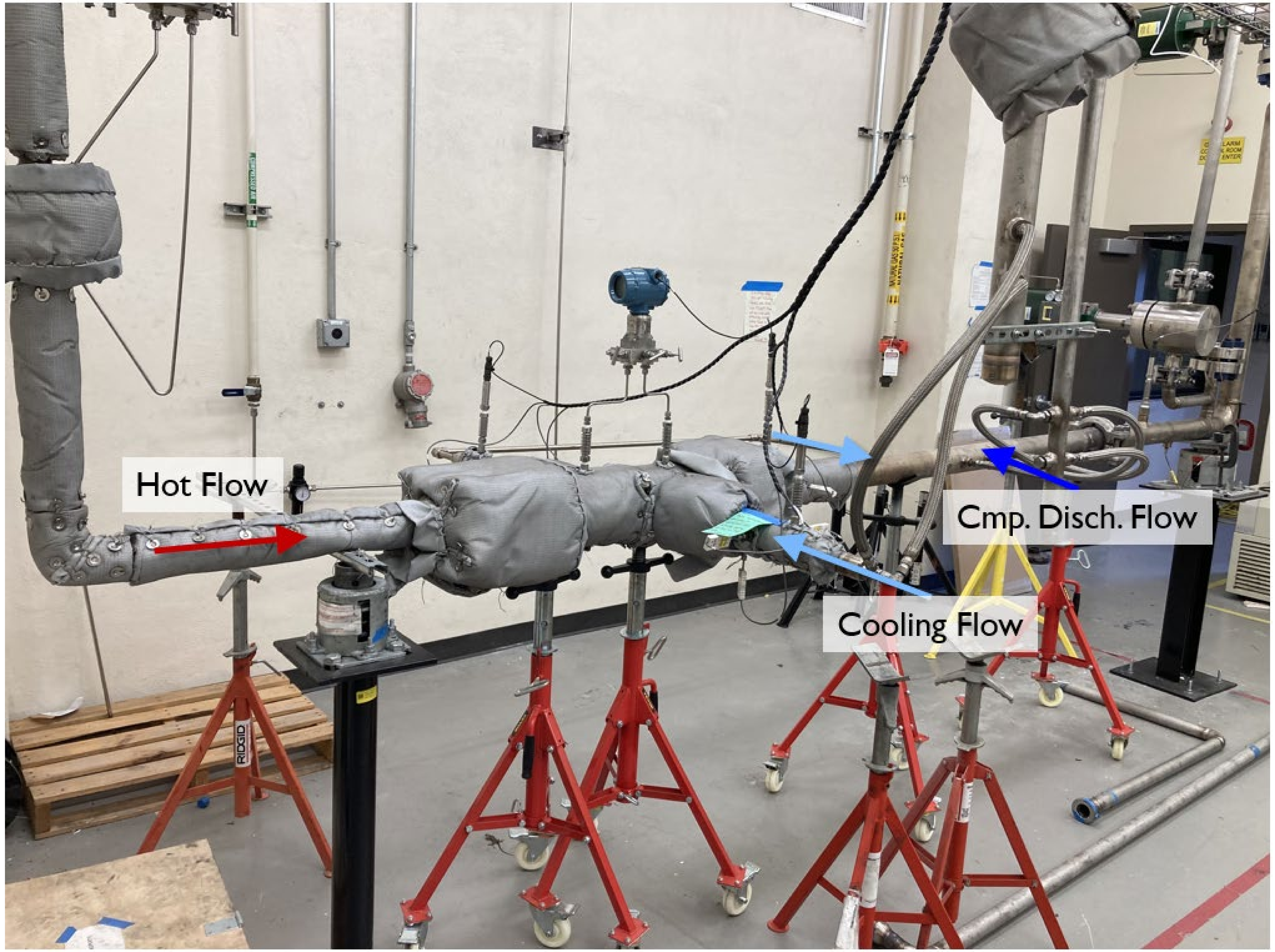

Test Section Design

- Features two symmetric flow serpentine pathways, each with five passes.
- Aspect ratio chosen based on a half passage height due to capability of manufacturing ribs on only one wall.
- Parameters chosen based on common design practice and details of 1st stage turbine blade for 300 MWe sCO_2 direct-fired turbine.

Parameter	Value
Rib height to hydraulic diameter (e/D_h)	0.076
Rib pitch to rib height (p/e)	10
Rib chevron (V) angle	45 deg.
Passage length to hydraulic diam. ratio (L/D_h)	10
Passage aspect ratio (w/h)	1

Test Section Design

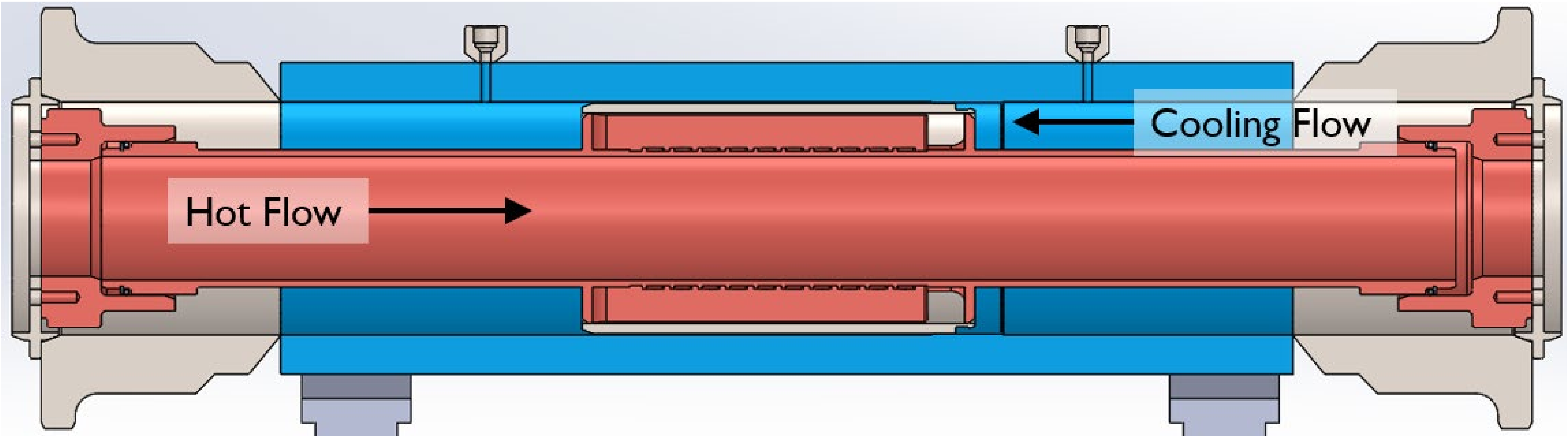

- Outer case designed to 250 bar, 537°C with the intent of ASME BPVC Section VIII, Div 2.
- Metallics seals and PTFE spring-energized seal used to prevent flow-mixing and any leakage around serpentine section.

Data Reduction

- Goal of test operation: Collect data at varying RE number for the cooling flow and capture the fluid thermal resistance and pressure drop to be able inform quantities of interest.
  - Nusselt number enhancement ratio (Nu/Nu_0), relative to smooth wall analytical value.
  - Friction factor ratios (f/f_0), relative to smooth wall analytical value.
- The cooling flow mass flow rate, and therefore RE number, was modified through manipulation of a control valve on the heater bypass line.
- To isolate the heat transfer characteristics of the cooling flow, a modified Wilson plot technique was employed similar to the implementation used in sCO_2 heat transfer experiments by Searle et al. [8].

Data Reduction - Continued

$$RE = \frac{\dot{m}_c D_{passage}}{2\mu(T_c, P_c) A_{passage}}$$

$$R_{total} = \frac{\Delta T_{LMTD}}{q} = \frac{\frac{\left((T_{h,in} - T_{c,out}) - (T_{h,out} - T_{c,in})\right)}{ln(\frac{T_{h,in} - T_{c,out}}{T_{h,out} - T_{c,in}})}}{\dot{m}_c\left(h(T_{c,in}, P_{c,in}) - h(T_{c,out}, P_{c,out})\right)}$$

$$R_{total} = R_{t,c} + R_{t,w} + R_{t,h}$$

$$R_{total} = m(\frac{1}{Re^{0.8} Pr^{0.4} k}) + (R_{const}), of\ form\ y = mx + b$$

$m \equiv$ slope of Wilson plot

$$R_{const} = R_{t,w} + R_{t,h}$$

$$R_{t,c} = R_{total} - R_{const} = \frac{1}{UA_{eff}} \rightarrow U = \frac{1}{R_{t,c} A_{eff}}$$

$$Nu = \frac{UD_h}{k}$$

- The modified Wilson plot method leverages the test points of the smooth wall insert to calculate the constant thermal resistance contribution, with hot flow conditions kept constant.
- The cooling flow thermal resistance can be isolated for each test point from the measured overall thermal resistance, and an overall heat transfer coefficient (U) and Nusselt number extracted.

Data Reduction - Continued

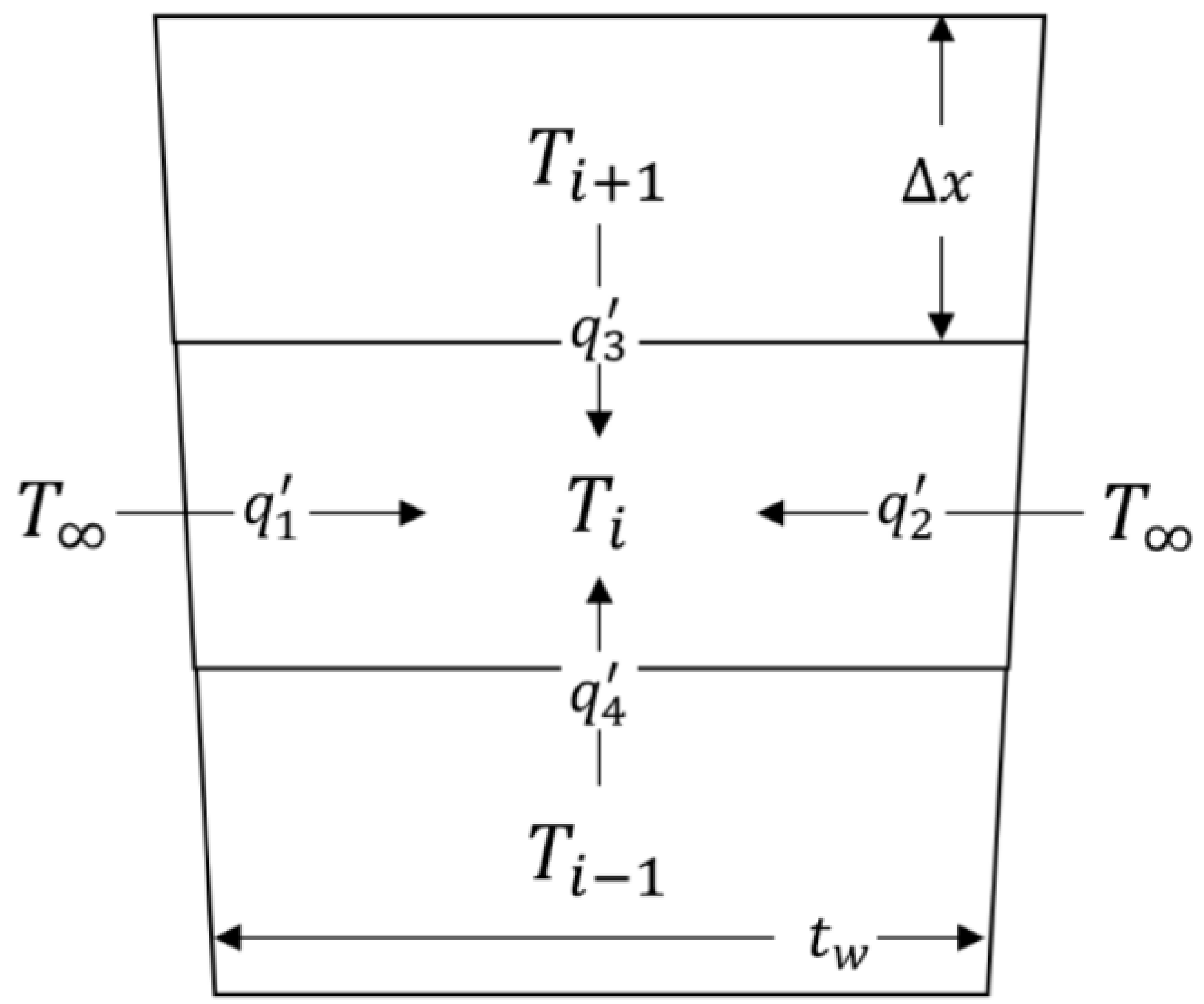

$$q_1' = U\Delta x(T_\infty - T_i)$$

$$q_2' = U\Delta x(T_\infty - T_i)$$

$$q_3' = \frac{kt_w(T_{i+1} - T_i)}{\Delta x}$$

$$q_4' = \frac{kt_w(T_{i-1} - T_i)}{\Delta x}$$

$$\left(\frac{kt_w}{\Delta x}\right)T_{i-1} + \left(-\frac{2kt_w}{\Delta x} - 2U\Delta x\right)T_i + \left(\frac{kt_w}{\Delta x}\right)T_{i+1} = -2U(\Delta x)T_\infty$$

$$\begin{bmatrix} 1 & \cdots & a_{1n} \\ \vdots & \ddots & \vdots \\ a_{n1} & \cdots & a_{nn} \end{bmatrix} \begin{bmatrix} T_1 \\ T_i \\ T_n \end{bmatrix} = \begin{bmatrix} T_{base} \\ b_i \\ b_n \end{bmatrix}$$

$$R_{t,c} = R_{total} - R_{const} = \frac{1}{UA_{eff}} \rightarrow U = \frac{1}{R_{t,c}A_{eff}}$$

$$Nu = \frac{UD_h}{k}$$

- When calculating the Nusselt number, the effective area must be accounted for due to passage dividing walls seeing a decreasing temperature potential between wall and fluid temperature. A_{eff} is a function of U.
- A discretized passage diving wall model is used to form its temperature profile. An iterative solver finds the single unique value for U at each test point that satisfies the cooling fluid thermal resistance calculated.

Data Reduction - Continued

$$f_0 = (0.790\ln(Re) - 1.64)^{-2}$$

$$Nu_0 = \frac{\left(\frac{f_0}{8}\right)(Re-1000)Pr}{1+12.7\left(\frac{f_0}{8}\right)^{\frac{1}{2}}\left(Pr^{\frac{2}{3}}-1\right)}$$

- The smooth wall values for friction factor and Nusselt number are found from Petukhov and Gnielinski correlations [14].

$$k = \frac{\Delta P}{P_{dyn}}$$

$$f = \frac{(\Delta P - 4k_{turn}P_{dyn})D_h}{P_{dyn}L_{total}}$$

$$P_{dyn} = \frac{\left(\frac{\dot{m}_c}{2A_{passage}}\right)^2}{2\rho}$$ $\equiv$ passage dynamic pressure

k_{turn} $\equiv$ loss factor assumed for each tip turn, four in total.

- An overall k-factor normalizes the pressure loss across the entire serpentine section by the passage dynamic pressure.
- The friction factor is calculated by separating out the tip turn flow-turning losses, to match its classical definition as commonly used in literature.

Data Reduction - Continued

- Error propagation methods of bias and precision uncertainty are used, in accordance with ASME Journal of Heat Transfer guidelines [15].
- Bias limit values based on:
  - Multi-point calibrated RTDs and TCs uncertainty.
  - Differential pressure transmitter uncertainty.
  - Orifice plate discharge coefficient uncertainty.
- Precision limit based on unsteadiness in process variables during 30-second averages taken (1 sample per second).
  - Calculated as 2σ (2x standard deviation) of the reported variable.
- To uncertainty of the assumed constant thermal resistance contribution of the hot flow is calculated by 2σ of the estimated hot fluid thermal resistance values over the 30-second average. These variations are captured through use of the Dittus-Boelter scaling laws.

Results

- Targeted inlet state points above 150°C for a lower specific heat than the maximum seen at lower temperatures at a 200 bar isobar, and maintained a temperature difference between the two streams of approximately 200°C to generate a significant temperature delta across the test section.
- When charts of cooling flow inlet temperature and total thermal resistance were observed to oscillate around a near constant value, a 30 second averaging of the data was taken and registered as a test point. With each adjustment in loop controls to arrive at a new Reynolds number, typical spans of 10-15 minutes were used between the registering of test points.

Parameter	Minimum value	Maximum value
Cooling Flow Inlet Pressure (bar)	183	205
Hot Flow Inlet Pressure (bar)	184	205
Cooling Flow Inlet Temperature (°C)	165	192
Cooling Flow Outlet Temperature (°C)	209	239
Hot Flow Inlet Temperature (°C)	402	418
Cooling Flow Mass Flow Rate (kg/s)	0.108	0.380
Hot Flow Mass Flow Rate (kg/s)	1.43	1.49

Results – total thermal resistance

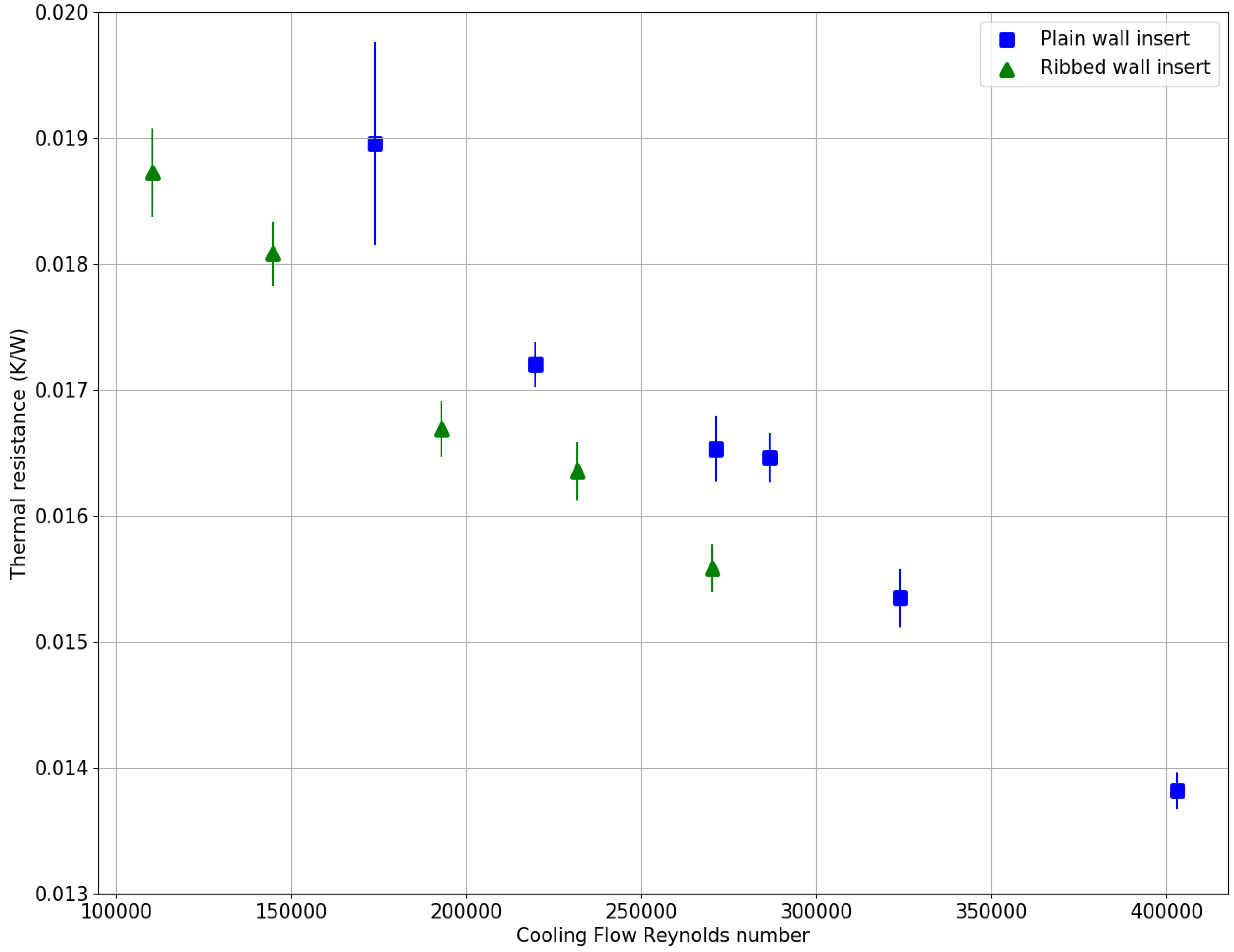

Results – Nusselt number

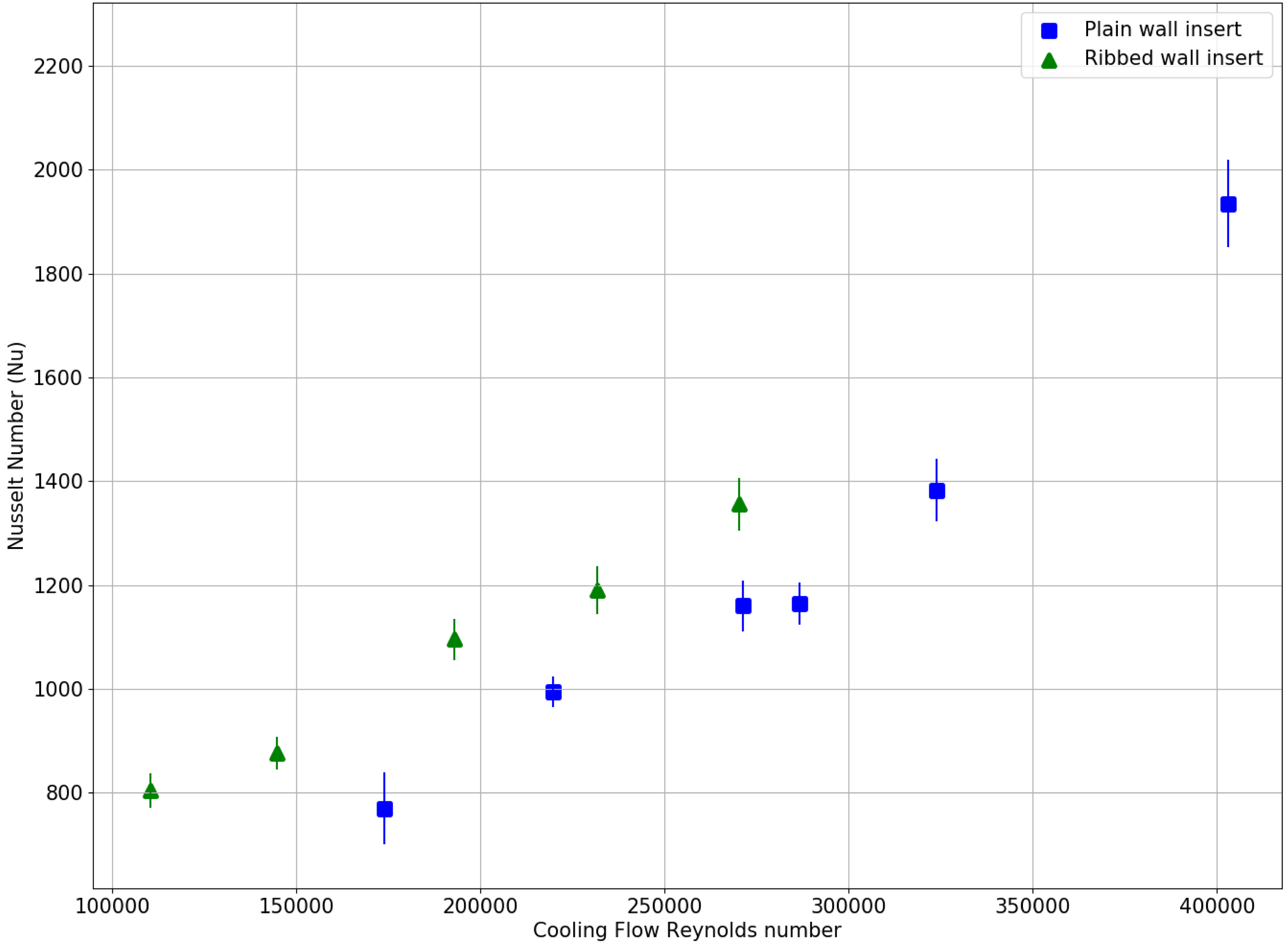

Results - commentary

- For both inserts, the thermal resistance decreases with increasing Reynolds numbers which, agreeing with the positive correlation between Nusselt number and Reynolds number seen in turbulent flow correlations.
- The ribbed insert demonstrated lower thermal resistance at test points at similar Reynolds number compared to the plain wall insert. This demonstrates the predicted effect of chevron ribs generating turbulence and increased flow mixing, thereby increasing heat transfer and registering the lower fluid thermal resistance relative to the plain wall.

Results – Nusselt number enhancement ratio

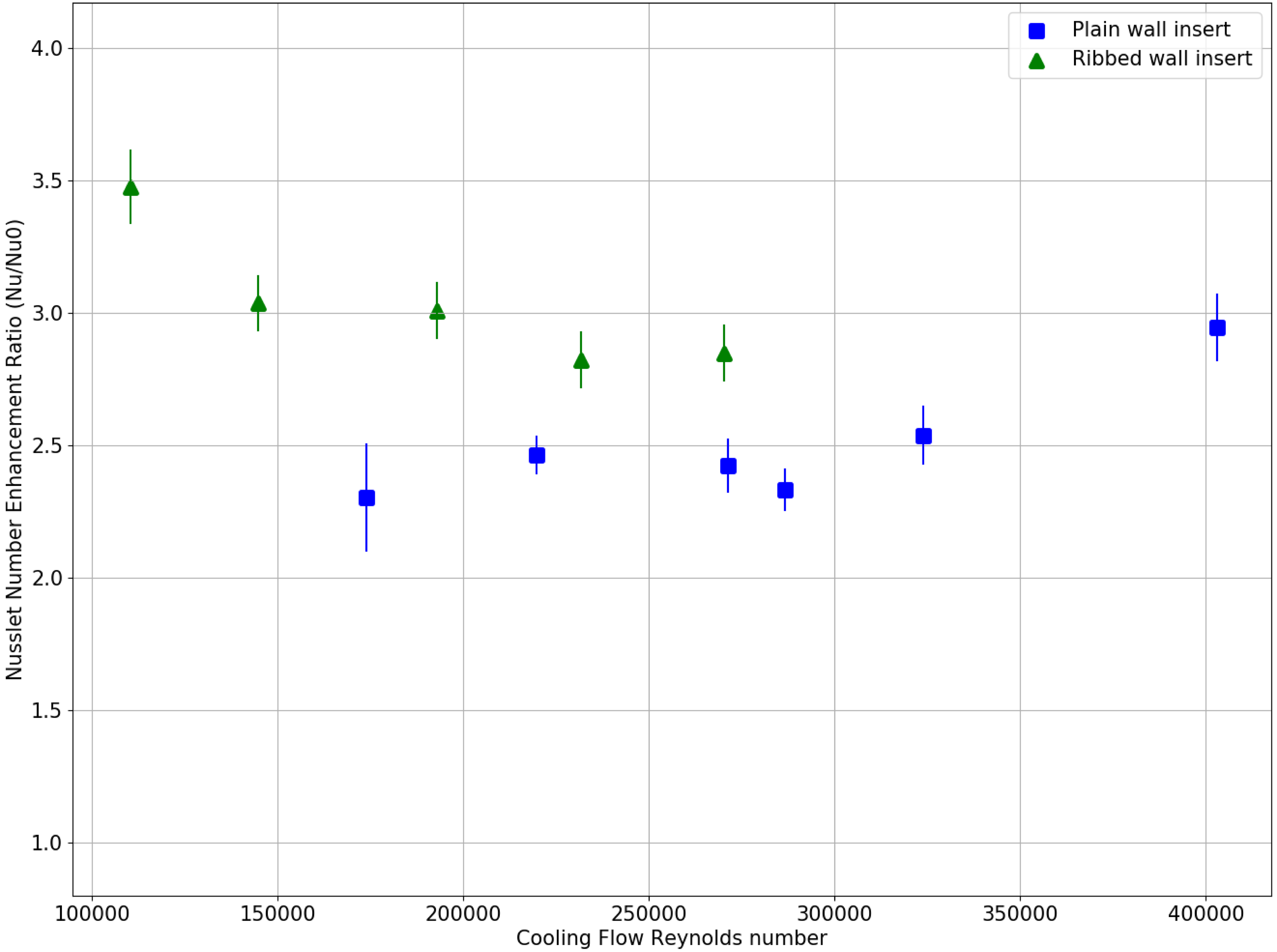

Results - commentary

- For the Reynolds number range between 150,000 and 300,000 where at least three test points were registered for both inserts, the ribbed wall data points average a Nu/Nu_0 of 2.90 while the plain wall data points have an average of 2.39.
- Though the ribs are the source of a comparatively higher Nusselt enhancement ratio, the plain wall still registers a significantly higher Nusselt number compared to a smooth wall calculation. This is anticipated to be due to the inherent surface roughness of the machined flow path, and also the effect that the 180 deg. tip turns have in promoting turbulence.

Results – Overall k-factor for pressure drop

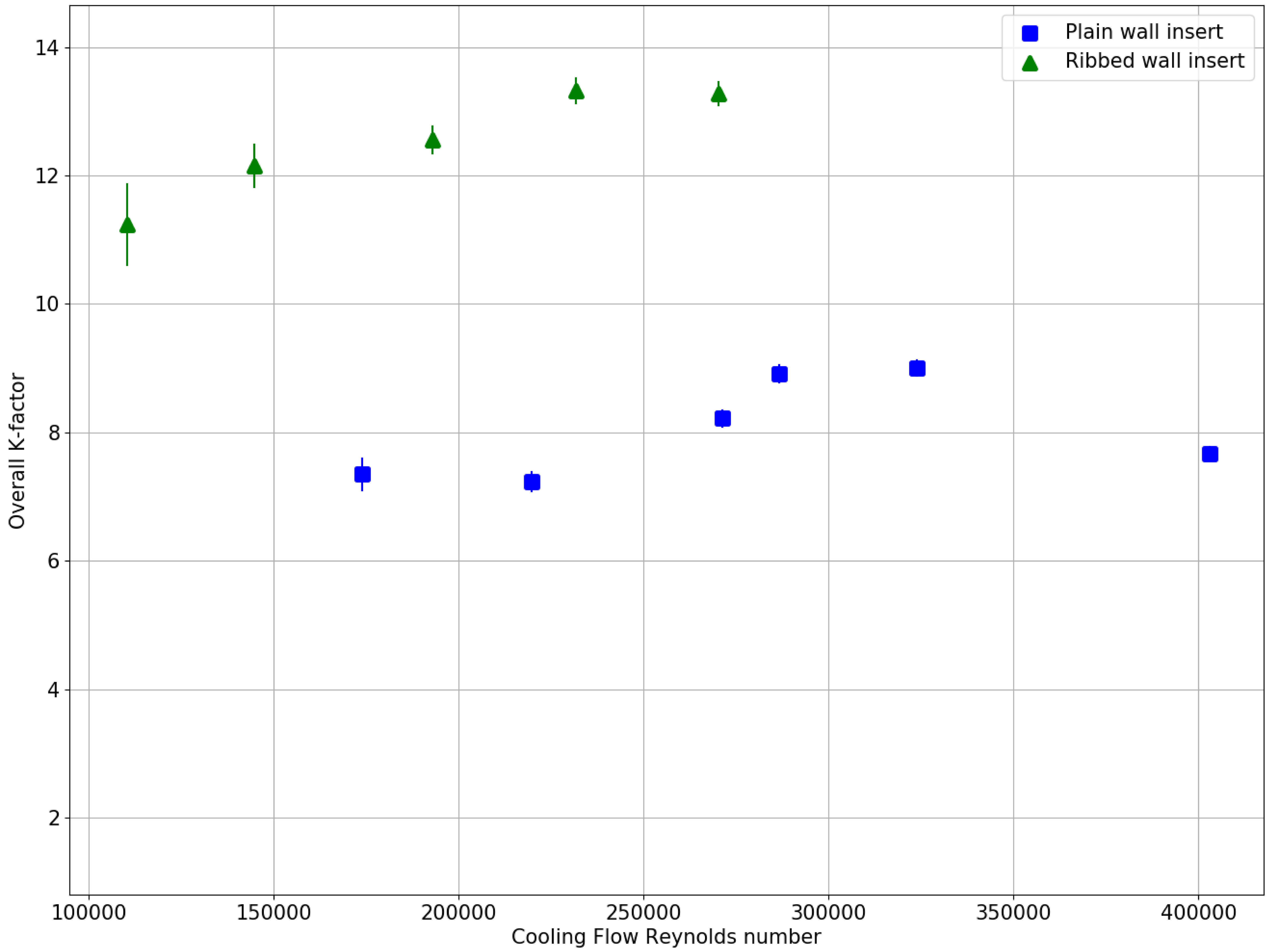

Results - commentary

- As expected, the additional enhancement of the ribbed wall geometry came with significantly greater pressure loss due to phenomena including the periodic separation from each rib.
- When compensating for an assumed loss factor of 1.5 times the dynamic pressure at each tip turn, f/f_0 for the ribbed wall insert ranges between 5.9 at the lowest Reynolds number and 9.8 at the highest Reynolds number.

$$f = \frac{(\Delta P - 4k_{turn}P_{dyn})D_h}{P_{dyn}L_{total}}$$

$$P_{dyn} = \frac{\left(\frac{\dot{m}_C}{2A_{passage}}\right)^2}{2\rho} \equiv \text{passage dynamic pressure}$$

k_{turn} $\equiv$ loss factor assumed for each tip turn, four in total.

Friction factor ratios of up to 10 can be expected for a chevron ribbed passage with characteristics aligned with those enumerated in Table 1, with the exact values depending on the relative losses of the straight passage and due to tip turns.

Conclusions

- When predicting heat transfer characteristics for midsection ribbed, serpentine internal cooling passages, Nusselt number enhancement ratios near 3 can be expected based on the test data generated at pertinent Reynolds numbers for sCO_2. It is hypothesized that this outcome from the testing was due in a significant part to the inclusion of multiple tip turns through a serpentine path geometry.
- Friction factor ratios of up to 10 can be expected for a chevron ribbed passage with characteristics aligned with those used for testing, with the exact values depending on the relative losses of the straight passage and due to tip turns.
- The case can be made that less penalty should be ascribed to the pressure losses for internal cooling geometry relative to a gas turbine.
  - Due to the large pressure difference across the first stage blade for a sCO_2 turbine in direct-fired application, a significant pressure differential is accessible between the internal cooling flow pressure and the external flow path pressure.
  - Due to the high density of sCO_2 there can be a significant increase in total pressure for flow through an internal cooling passage traveling from hub to tip due to blade rotation (pumping effect).

References

[1] Weiland, N.T., & White, C.W. (2019). *Performance and Cost Assessment of a Natural Gas-Fueled Direct sCO2 Power Plant*. NETL-PUB-22274. https://doi.org/10.2172/1503567.

[2] 8 Rivers Capital. *Allam Cycle Zero Emission Coal Power: Design Basis, Final Report*. Reference Number 89243319CFE000015.

[3] Wardell, R., Richardson, J., Otto, M., Smith, M., Fernandez, E., Kapat, J. (2023). "An Experimental Investigation of Heat Transfer for Supercritical Carbon Dioxide Cooling in a Staggered Pin Fin Array". *Proceedings of the ASME Turbo Expo 2023: Turbomachinery Technical Conference and Exposition*. GT2023-103263.

[4] Richardson, J., Wardell, R., Fernandez, E., Kapat, J.S. (2023). "Experimental and Computational Heat Transfer Study of sCO_2 Single-jet Impingement". *Proceedings of the ASME Turbo Expo 2023: Turbomachinery Technical Conference and Exposition*. GT2023-102544.

[5] Wright, L.M., Fu, W.L., Han, J.C. (2004). "Thermal Performance of Angled, V-Shaped, and W-Shaped Rib Turbulators in Rotating Rectangular Cooling Channels (AR=4:1)". *ASME Journal of Turbomachinery*. Vol. 126, pp. 604-614.

[6] Wieler, M., Woerz, B., Jeschke, P., Rabs, M. (2019). "Thermal Performance of Angled, V-Shaped, and W-Shaped Rib Turbulators in Rotating Rectangular Cooling Channels (AR=4:1)". *ASME Journal of Turbomachinery*. Vol. 126, pp. 604-614.

[7] Han, J.C., Dutta, S., Ekkad, S. (2013). *Gas Turbine Heat Transfer and Cooling Technology, 2nd Edition*. Section 4.2.10. CRC Press.

[8] Searle, M., Roy, A., Black, J., Straub, D., Ramesh, S. (2021). "Investigating Gas Turbine Internal Cooling Using Supercritical CO_2 at High Reynolds Numbers for Direct Fired Applications". *Proceedings of the ASME Turbo Expo 2021: Turbomachinery Technical Conference and Exposition*. GT2021-59630.

[9] Wilkes, J., Robinson, K., Wygant, K., Pelton, R., Bygrave, J. (2022). "Design and Testing of a 275 bar 700 degree Celsius Expander for an Integrally Geared Supercritical CO2 Compander". *Proceedings of the ASME Turbo Expo 2022: Turbomachinery Technical Conference and Exposition*. GT2022-83284.

[10] Moore, J., Cich, S., Day, M., Allison, T., Wade, J., Hofer, D. (2018). "Commissioning of a 1 MWe Supercritical Test Loop". *Proceedings of the 6th International Supercritical CO_2 Power Cycles Symposium.*

[11] Rau, G. Cakan, M., Moeller, D., Arts, T. (1996). "The Effect of Periodic Ribs on the Local Aerodynamic and Heat Transfer Performance of a Straight Cooling Channel". *Proceedings of the International Gas Turbine and Aeroengine Congress & Exposition.* 96-GT-541.

[12] Chandra, P.R., Niland, M.E., Han, J.C. (1996). "Turbulent Flow Heat Transfer and Friction in a Rectangular Channel with Varying Number of Ribbed Walls". *Proceedings of the International Gas Turbine and Aeroengine Congress & Exposition*. 95-GT-13.

[13] ASME. (2013). ASME Boiler and Pressure Vessel Code Section VIII-Rules for Construction of Pressure Vessels. New York.

[14] Incropera, F.P., Dewitt, D.P., Bergman, T.L., Lavine, A.S. (2007). *Fundamentals of Heat and Mass Transfer, 6th ed.* John Wiley & Sons.

[15] ASME International. "Policy on Reporting Uncertainties in Experimental Measurements and Results". Journal of Heat Transfer Policy.

QUESTIONS